

<http://ansinet.com/itj>

ITJ

ISSN 1812-5638

INFORMATION TECHNOLOGY JOURNAL

ANSI*net*

Asian Network for Scientific Information
308 Lasani Town, Sargodha Road, Faisalabad - Pakistan

A Novel Pavement Distress Image Filtering Algorithm

¹Shen Yu, ¹Dang Jian-Wu, ²Feng Xin and ¹Wang Yang-Ping

¹School of Electronic and Information Engineering, Lanzhou Jiaotong University, Lanzhou, 730070, China

²College of Mechanical Engineering, Chongqing Technology and Business University,
Chongqing, 400067, China

Abstract: Combined the Nonsubsampled Contourlet Transform (NSCT) with compressed sensing de-noising theory, this study proposed a compressed sensing image filtering algorithm in the NSCT transform domain. This algorithm adopted the transform domain filtering method. Firstly, the NSCT was used to do multi-scale and multi-directional transform on the input noisy pavement distress Image which was mapped to the transform domain. Then the compressed sensing theory was used to filter the high-frequency sub-band coefficients. The experiment results show that this algorithm improves the effectiveness and timeliness of the pavement distress image filtering.

Key words: Transform domain, compressed sensing, pavement distress image

INTRODUCTION

Designing fast and efficient pavement distress image filtering algorithm is the cornerstone of the pavement distress automatic detection technology. Transform domain filtering (Sheng *et al.*, 2012; Xiao *et al.*, 2009) is common in the pavement distress image filtering. The familiar transform methods are the Fourier transform and wavelet transform. The pavement cracks extract comes into the domain of one-dimensional singularity detection in the two-dimensional images. In the representation of the one-dimensional singularity, neither of the wavelet basis and Fourier basis is the optimal basis. They could not depict the edge continuity. Many researches focused on the Multiscale Geometric Analysis filtering method. Wang *et al.* (2007) proposed pavement image denoising algorithm in Curvelet domain (Candes and Donoho, 1999). It synthesizes the advantages that Ridgelet is good at line feature representation and wavelet is good at point feature representation. It achieved good effect in the reticular cracks image de-noising. Da Cunha *et al.* (2006) advanced the Nonsubsampled Contourlet Transform (NSCT). Not only do NSCT inherit the merits of capturing line singular feature from the Contourlet transform but also it has absolute translation invariance.

On top of that, compressed sensing (Tsaig and Donoho, 2006) (CS) proposed in 2006, gained favorable results in the signal de-noising. Donoho (2006) mentioned Compressed Sensing De-noise (CSDN) method. CSDN indicated that Basis Pursuit (BP) can be used to suppress

noise by modifying the constraint conditions when the noise distribution is known.

The Nonsubsampled Contourlet Transform (NSCT) has the translation invariant feature and good image line singular characteristics capture feature. The compressed sensing theory has effective noise suppression capability. On the basis, this study proposed a novel compressed sensing filtering algorithm in NSCT transform domain.

Nonsubsampled contourlet transform: The NSCT has all of the characteristics of Contourlet transformation. On top of that, it is also translation invariant. So it effectively reduces the influence which the image registration error over the fusion results. The image transformed by the NSCT has the same size with the original image. So NSCT is suitable to image fusion.

Similar to the Contourlet transformation, the scale decomposition and the direction decomposition (Xiao *et al.*, 2011) are treated separately in the NSCT. On the first step, the Nonsubsampled Pyramid Filter Bank (NSPFB) is used to do multi-scale decomposition on the original image. On the second step, the Nonsubsampled Directional Filter Bank (NSDFB) is used to do directional decomposition on the multi-scale sub-band images. It is shown as Fig. 1 (Qingqing *et al.*, 2011). The low-frequency image is produced by convolving the input image with a two-dimensional filter. The difference between the original image and the low-frequency image is the high-frequency detail image. On the third step, the high-frequency detail image directional details are produced by the NSDFB. After N-level NSCT decomposition:

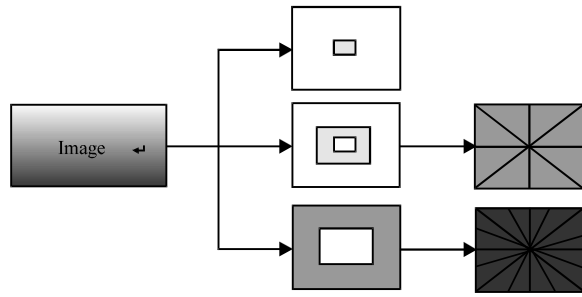


Fig. 1: NSCT block diagram

$$1 + \sum_{j=1}^N 2^{lj}$$

sub-band images are got, where l_j is the direction decomposition levels on j scale.

Compressed sensing: The compressed sensing theory denotes that the input signal is sparse in the sense, meaning that it essentially depends on a number of degrees of freedom which is smaller than the original signal length. So this study introduced the sparse representation to fuse images. The steps of the compressed sensing are the sparse representation, random measurement and reconstruction. The sparse representation is the prerequisite of compressed sensing. The random measurement is the key condition to realize reconstruction. And the reconstruction is an optimization process to obtain the idea results.

For the compressed sensing de-noising method, the sparse representation is required at first. In the compressed sensing theory, the original signals must be sparse in one certain transformed domain. The existence of the noise destroys the sparse of the signal in the transform domain. So the method reconstructs the sparse representation of the clean image to achieve the aim of filtering.

Suppose x is a one-dimensional signal which is N in length. Its sparsity is k . That is, there are k non-zero values in this signal. The signal is sparse represented on one certain sparse basis:

$$x = \Psi s \tag{1}$$

where, Ψ is the sparse matrix. s is the sparse coefficient.

In the compressed sensing theory, it need design the observation matrix Φ after the sparse representation. The effect of the observer is to sample M observation values and assure reconstructing original signals from these values.

Compressed sensing observes the signal x by the $m \times n$ observation matrix Φ to get the observation value y :

$$y = \Phi \cdot x \tag{2}$$

The compressed sensing is come down to the following problem:

On the basis of the observation value y and observation matrix Φ , resolve the under determined equations $y = \Phi x$ to obtain the original signal x . In the end, the process is transformed to optimization problem:

$$\hat{x} = \operatorname{argmin} \|x\|_0 \quad \text{s.t. } y = \Phi x \tag{3}$$

The process is called reconstruction.

Steps of this algorithm: A noisy pavement distress image was decomposed to low-frequency sub-band coefficients and high-frequency sub-band coefficients after the NSCT. The high-frequency sub-ban coefficients were sparse signals and low-frequency sub-band coefficients were approximation signals with little sparse. The frequency coefficients of the original image are concentrated in the low-frequency domain. And the frequency coefficients of the noise are concentrated in the high-frequency domain. The de-noised image can be got after treating the high-frequency coefficients. In this study, the high-frequency coefficients were filtered by the compressed sensing method.

The steps of this de-noising method are shown as follows (Yin *et al.*, 2010):

- Step 1:** The input noisy pavement distress image was decomposed to the low-frequency coefficients and high-frequency coefficients by the NSCT
- Step 2:** For the high-frequency sub-band coefficient, pseudo-random Fourier matrix was used as the observation matrix to get the observation values
- Step 3:** For the observation values, split Bergman iteration method was used to reconstruct the optimal coefficients
- Step 4:** Reconstruct the optimal high-frequency sub-band coefficients and low-frequency sub-band coefficients to get the filtered pavement distress image by the inverse NSCT

PROPOSED ALGORITHM

Compressed sensing de-noising algorithm: The low-frequency sub-band coefficients cover most energy of the noisy image. They are the mappings of the image contour. The high-frequency sub-band coefficients mainly represent the image details, texture information and noise. They are sparse to some extent. After transformed

by the Directional Filter Bank, the high-frequency coefficients are much sparse. They satisfy the compressed sensing theory.

High-frequency sub-band coefficients observation:

Pseudo-random Fourier matrix was used to observe the Tetrolet coefficients which is shown in Fig. 2. Pseudo-random subsampling is polynomial variable density sampling. It obeys the probability density function law that intensive sampling in the low-frequency component and sparse sampling in the high-frequency component. In this study, the sparse sampling was needed in the high-frequency. So the Pseudo-random Fourier matrix observation could greatly reduce the complexity of the following optimization algorithm:

$$G_{lm} = I_{lm} * f, n = 1, 2, \dots, 12 \quad (4)$$

where, f is the pseudo-random Fourier matrix. G_{lm} is the Tetrolet observation value.

High-frequency sub-band coefficients reconstruction:

Split Bergman iteration method is a kind of efficient iterative method in literature (Goldstain and Osher, 2009). It performs well in optimization problems with L_1 . The programming of the algorithm is simple. Its solution performance is stable. The regularization parameter is a constant. Moreover, this algorithm occupies smaller memory and has fast computing speed and convergence rate.

The core of the high-frequency observation values reconstruction is to resolve the optimization problem:

$$\min_{x \in \mathbb{R}^n} \sum |\Psi x|, \quad \text{s.t. } \phi x = y \quad (5)$$

where, Ψ is the sparse transform matrix. In this study, it was $\Psi = g_i * W^{(m)}$. x is the sparse form of the signal. ϕ is the observation matrix. In this study, it was $\phi = T$. Y is the observation values. In this study, it was $y = G_{lm}$.

According to literature (Plonka, 2011), the simplified split Bergman formulas are:

$$\begin{cases} (x^{k+1}, y^{k+1}) = \arg \min \left\{ E(x, y) + \frac{\mu}{2} \|y - \Psi x - b^k\| \right\} \\ b^{k+1} = b^k + \Psi x^{k+1} - y^{k+1} \end{cases} \quad (6)$$

For the minimization of equation (6), interactive split Bergman iteration method was used to get the following equation:

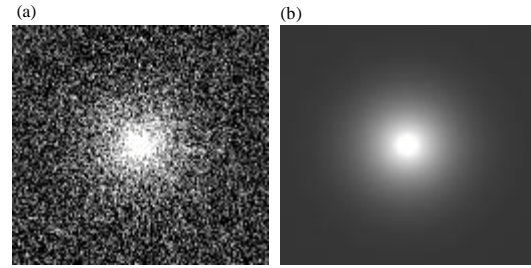


Fig. 2(a-b): Observation matrix. (a) Fourier domain sampling model and (b) Two-dimensional probability density function

Table 1: Split Bergman iterative algorithm processes

Input: $(x^0, y^0, b^0) = (0, 0, 0)$	
While do not meet the stop condition	
Step1:	$x^{k+1} = \frac{1}{2\mu+1} \Phi f + \frac{1}{2} \left(I_N - \frac{1}{2\mu+1} \Phi^T \Phi \right) (\Psi^T (y^k - b^k))$
Step2:	$y^{k+1} = \Gamma \mu^{-1} \wedge (\Psi x^{k+1} + b^k)$
Step3:	$b^{k+1} = b^k + \Psi x^{k+1} - y^{k+1}$
End	

$$\begin{cases} x^{k+1} = \arg \min_x \left\{ \frac{1}{2} \|f - \Phi x\|_2^2 + \frac{\mu}{2} \|y^k - \Psi x - b^k\| \right\} \\ y^{k+1} = \arg \min_x \left\{ \|\wedge y\| + \frac{\mu}{2} \|y - \Psi x^{k+1} - b^k\|_2^2 \right\} \\ b^{k+1} = b^k + \Psi x^{k+1} - y^{k+1} \end{cases} \quad (7)$$

The flow of the algorithm is shown as Table 1.

This algorithm did not need resolve the linear system equations, just the x^{k+1} . The step 2 and 3 were processed in the coefficients domain. Where, x^{k+1} denotes the optimal high-frequency coefficient which was reconstructed by $k+1$ Bergman iteration.

The compressed sensing reconstructed results of the third layer coefficients components were obtained by superimposing the 3 group reconstructed coefficients in the third layer. The compressed sensing reconstructed results of the first and second layer coefficients were got in the same manner.

Image reconstruction: Finally, reconstruct the optimal high-frequency sub-band coefficients and low-frequency sub-band coefficients to get the filtered pavement distress image F by the inverse NSCT.

Experiment results and analysis: The captured pavement distress images are usually affected by the scatter noises, such bitumen, pebbles and etc. So it is necessary to filter these images.

The experiments adopted the pavement distress images captured in the Wuwei city total line+S308-uplink-1 lane 3. The height of the CCD line scan camera was 2 m.

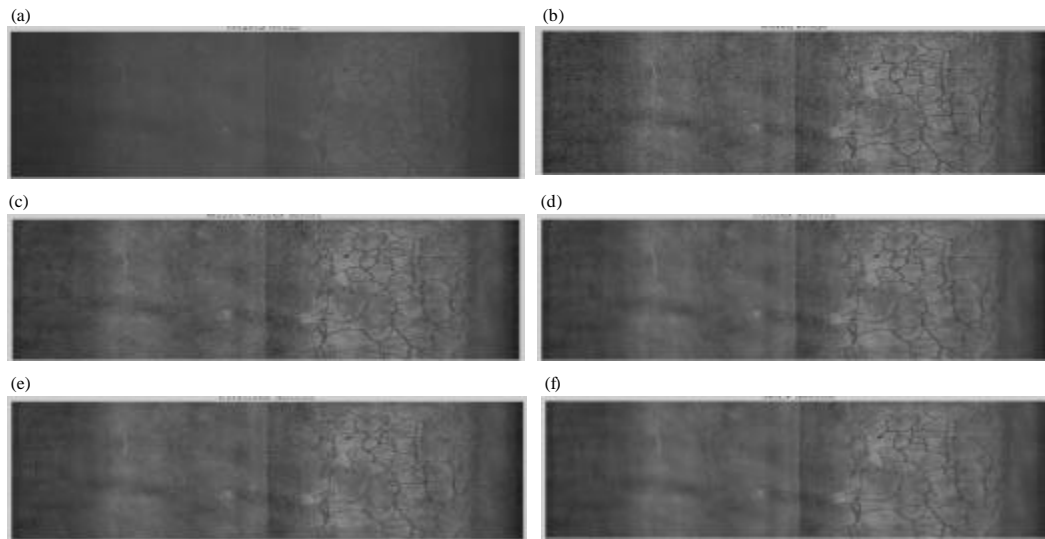


Fig. 3(a-f): Contrast of various methods. (a) Original pavement block crack image, (b) Adaptation histogram equalization, (c) Bayes wavelet denoising, (d) Curvelet denoising, (e) Contourlet hard threshold denoising and (f) Denoising algorithm in this study

The camera resolution was 1280*1024. The shooting angle was vertical. The speed of the car was 60 km h⁻¹. In the preprocessing, the original images were transformed to the PNG form and 512*512 size. Then the PNG images were adaptive histogram equalized.

The experiments compared the algorithm in this paper with three existing de-noising algorithm which were Bayes Wavelet de-noising, Curvelet de-noising and Contourlet hard threshold de-noising. For the subjective evaluation, the experiments compared the de-noised image quality. For the objective evaluation, the computing times were compared to verify the performance of these algorithms.

The experiment results are shown in Fig. 3.

Figure 3a is the original pavement block split image. There are many singular points besides and far off the crack. Figure 3b is the adaptive histogram equalization image. It enhanced the contrast to favor for the further processing. Figure 3c is the de-noised image by the Bayes wavelet. It could effectively constrain the scatter noise. But the abstracted cracks were a range of discontinuous spots which cannot proceed any further. Figure 3d is the de-noised image by the Curvelet hard threshold. It better restrained the scatter noise and remained the edge contour. Figure 3e is the de-noised image by the Contourlet transform hard threshold. Its 4 decomposition scales were 8, 8, 16, 16 and decomposition direction from coarse to fine. Its directional filter bank is the 'pkva' and pyramid filter bank is '9-7'. The Contourlet transform represented the local linear structure information by the

sparse matrix. It clearly exhibited the crack by reserving the maximum coefficients and restraining the minimum coefficients in the sparse matrix. The maximum coefficients were the mapping of the crack and the minimum coefficients were the mapping of the noise. But the de-noised image lost some details and had certain distortion. Figure 3f is the de-noised image by the algorithm in this study. The visual effect of the reconstructed de-noised image is obvious better than the previous 3 results. It better filtered the scatter noise. At the same time, it reserved the crack structure and detail information to the greatest degree. It also removed most singular points which cannot be wiped off by the Curvelet and Contourlet method.

Furthermore, the de-noising time of these 4 methods was calculated. The method in this study spent the shortest time that 1.1640s. The Curvelet method spent the longest time that 15.1642s.

In a few words, Bayes Wavelet had fast computing speed but the worst quality. Curvelet method spent the longest time. The algorithm in this study has the fastest computing speed and the best de-noise effect in the four methods. It has obvious predominance in the pavement distress image de-noise application.

CONCLUSION

The study adopted the compressed sensing filtering algorithm in the NSCT domain to de-noise the pavement

distress images. Compared with the Wavelet, Contourlet and Curvelet algorithm, it has lower redundancy and translation invariant. At the same time of reserving the crack structure and detail information to the greatest degree, it better filtered the scatter noise. The experiment results show that this algorithm is better than the traditional algorithms in the pavement image de-noising. It not only has good computing speed but also better represents the edge information and detail features of the image.

ACKNOWLEDGMENT

Project was supported by National Natural Science Foundation of China (60962004 and 61162016) and Lanzhou Jiaotong University Young Scholar Fund (2012003).

REFERENCES

- Candes, E.J. and D.L. Donoho, 1999. Curvelets, a surprisingly effective no adaptive representation for objects with edges. Proceedings of the 4th International Conference on Curve and Surface. July 1-7, 1999, Vanderbilt University Press, Saint-Malo, France pp: 105-120.
- Da Cunha, A.L. J. Zhou and M.N. Do, 2006. The nonsubsampling contourlet transform: Theory, design and applications. *IEEE Trans. Image Process.*, 15: 3089-3101.
- Donoho, D.L., 2006. Compressed sensing. *IEEE Trans. Inform. Theory*, 52: 1289-1306.
- Goldstain, T. and S. Osher, 2009. The split bregman method for L1-regularized problems. *SIAM J. Imaging Sci.*, 2: 323-343.
- Plonka, G., 2011. Curvelet-wavelet regularized split bregman iteration for compressed sensing. *Int. J. Wavelets, Mul. Sol. Info. Proc.*, 9: 79-110.
- Qingqing, H., J. Yuan and Y. Jian, 2011. Improved fusion method for infrared and visible remote sensing imagery using NSCT. Proceedings of the 6th International Conference on Industrial Electronics and Applications, June 21-23, 2011, Beijing, China, pp: 1012-1015.
- Sheng, Y., L. Minggang, Y. Jianping and H. Chaohuan, 2012. Novel ultrasound image denoising method based on NSCT transformation. *Chinese J. Sci. Instru.*, 33: 1005-1012.
- Tsaig, Y. and D.L. Donoho, 2006. Extensions of compressed sensing. *Signal Processing*, 86: 549-571.
- Wang, G., X. Liang and H. Anzhi, 2007. Algorithm research of adaptive fuzzy image enhancement in ridgelet transform domain. *Acta Optica Sinica*, 27: 1183-1190.
- Xiao, Q., X. Ding, S. Wang, D. Guo and Y. Liao, 2009. Image denoising based on adaptive over-complete sparse representation. *Chinese J. Scient. Instrum.*, 30: 1886-1890.
- Xiao, Y.H., Z.H. Xi, T. Hai and L. Guo, 2011. Image edge detection based on nonsubsampling contourlet transform. *Syst. Engin. Elect.*, 7: 1668-1672.
- Yin, S., L. Cao, Q. Tan and G. Jin, 2010. Infrared and Visible Image Fusion based on NSCT and Fuzzy Logic. Proceedings of the International Conference on Mechatronics and Automation, August 4-7, 2010, Xi'an, pp: 671-675.